

# A Potential-Based Inversion of Unconfined Steady-State Hydraulic Tomography

by M. Cardiff<sup>1,2</sup>, W. Barrash<sup>3</sup>, P.K. Kitanidis<sup>2</sup>, B. Malama<sup>3</sup>, A. Revil<sup>4</sup>, S. Straface<sup>5</sup>, and E. Rizzo<sup>6</sup>

---

## Abstract

The importance of estimating spatially variable aquifer parameters such as transmissivity is widely recognized for studies in resource evaluation and contaminant transport. A useful approach for mapping such parameters is inverse modeling of data from series of pumping tests, that is, via hydraulic tomography. This inversion of field hydraulic tomographic data requires development of numerical forward models that can accurately represent test conditions while maintaining computational efficiency. One issue this presents is specification of boundary and initial conditions, whose location, type, and value may be poorly constrained. To circumvent this issue when modeling unconfined steady-state pumping tests, we present a strategy that analyzes field data using a potential difference method and that uses dipole pumping tests as the aquifer stimulation. By using our potential difference approach, which is similar to modeling drawdown in confined settings, we remove the need for specifying poorly known boundary condition values and natural source/sink terms within the problem domain. Dipole pumping tests are complementary to this strategy in that they can be more realistically modeled than single-well tests due to their conservative nature, quick achievement of steady state, and the insensitivity of near-field response to far-field boundary conditions. After developing the mathematical theory, our approach is first validated through a synthetic example. We then apply our method to the inversion of data from a field campaign at the Boise Hydrogeophysical Research Site. Results from inversion of nine pumping tests show expected geologic features, and uncertainty bounds indicate that hydraulic conductivity is well constrained within the central site area.

---

## Introduction

Traditional aquifer characterization techniques are generally based on assumptions of homogeneity (e.g.,

Theis' 1935 solution) or, in some cases, homogeneous anisotropy (Papadopoulos 1965) or simple layering (Hantush and Jacob 1955). However, the assumptions inherent in these methods and the meanings of the so-called average parameters they fit have come under scrutiny (Wu et al. 2005). In recent years, high-performance numerical models and developments in inverse theory have improved our ability to image subsurface heterogeneity through the use of techniques that are sensitive to aquifer heterogeneity and that integrate information from many pumping tests and many observation wells, that is, through inverse modeling. Data from several pumping tests can be combined and used in a tomographic fashion to characterize heterogeneity in the aquifer, a process known as hydraulic tomography (for recent field examples, see Bohling et al. [2007]; Li et al. [2007]; Straface et al. [2007]). Several techniques have been used to analyze data from hydraulic tomographic studies, including, among others, quasi-linear geostatistical techniques

---

<sup>1</sup>Corresponding author: Department of Civil and Environmental Engineering, Stanford University, Y2E2 Bldg., Rm. 161, 473 Via Ortega, m/c 4020, Stanford, CA 94305; (650)-723-4372; fax (650)-725-9720; mcardiff@stanford.edu

<sup>2</sup>Department of Civil and Environmental Engineering, Stanford University, Stanford, CA 94305.

<sup>3</sup>Department of Geosciences, Center for Geophysical Investigation of the Shallow Subsurface, Boise State University, Boise, ID 83725.

<sup>4</sup>Department of Geophysics, Colorado School of Mines, Golden, CO 80401.

<sup>5</sup>Dipartimento di Difesa del Suolo, Università della Calabria, Cosenza, Italy.

<sup>6</sup>Hydrogeophysics Laboratory, CNR-IMAA, Potenza, Italy.

Received June 2008, accepted December 2008.

Copyright © 2009 The Author(s)

Journal compilation © 2009 National Ground Water Association.  
doi: 10.1111/j.1745-6584.2008.00541.x

(Kitanidis and Vomvoris 1983; Kitanidis 1996; Snodgrass and Kitanidis 1998) and successive linear estimators (Yeh and Liu 2000; Liu et al. 2002; Zhu and Yeh 2005, 2006). Steady-state head data at points were used as the data in both these studies. Transient data are also useful, though in many cases there are too much data to practically analyze. Most studies inverting transient data apply a data reduction strategy to extract useful information from full drawdown curves—for example, by inverting temporal moments of head (e.g., Zhu and Yeh 2006) or through “steady shape” methods (Bohling et al. 2002, 2007). While hydraulic test data sets from fully screened wells can give good two-dimensional (2D) (depth averaged) estimates of aquifer properties, generally other data sources are required in order to resolve vertical variability. These supplementary data may come from a number of sources, including geophysical tests (Rubin et al. 1992; Copty et al. 1993; Hyndman et al. 1994; McKenna and Poeter 1995), borehole flowmeter logs (Li et al. 2008), or core samples (Illman et al. 2008). The depth-averaging properties of in-well instrumentation can also be overcome by using an array of sensors isolated at a variety of depths within a well, resulting in what is known as three-dimensional (3D) hydraulic tomography (Gottlieb and Dietrich 1995; Yeh and Liu 2000; Zhu and Yeh 2005). However, implementation of 3D hydraulic tomography at the field scale is still experimental (e.g., Butler et al. 1999; Barrash et al. 2007), and so far, most tests of 3D hydraulic tomography have been only at the laboratory scale (Liu et al. 2002, 2007; Illman et al. 2007).

In this article, we focus on the analysis of pumping test data from fully screened wells in unconfined aquifers to derive depth-averaged hydraulic conductivity distributions through inverse modeling. To simplify the numerical forward model, we develop a potential-based inversion approach that is independent of boundary conditions and natural sinks and sources within the domain under certain basic assumptions. We show through a numerical example that, using transformed measurements and linear error propagation, the best estimates and confidence intervals given by our method are acceptable.

Even with modern field equipment and computational resources, applications of inverse methods to hydrologic problems tend to be affected by a variety of complications and limitations. These include, among others, (1) suboptimal testing configurations and measurement strategies; (2) sparse, noisy measurements; (3) the influence of spurious unmodeled signals; (4) poorly characterized pretest conditions and/or boundary conditions; and (5) oversimplified numerical models. As part of this article, we also describe planning, design, and data analysis “best practices” that can help to alleviate these problems. Particularly, we argue that the use of conservative dipole pumping tests (for examples and references, see Luo et al. [2006]) has several advantages over traditional pumping-only tests in terms of both field implementation and modeling. Finally, we apply our methods to a field experiment carried out at the Boise Hydrogeophysical Research Site (BHRS) in 2007 and show how we have applied these principles to the design and analysis of our field experiment.

## Theory

### Mathematical Formulation

For ground water flow under steady-state unconfined conditions, subject to the Dupuit-Forchheimer assumption (i.e., horizontal bottom and minimal vertical flow), the hydraulic head field  $\phi_{\text{init}}$  satisfies:

$$N(\mathbf{x}) = \nabla \cdot (K\phi_{\text{init}}\nabla\phi_{\text{init}}) \quad \text{on } \Omega \quad (1)$$

where we assume Dirichlet boundary conditions:

$$\phi_{\text{init}} = f(\mathbf{x}) \quad \text{on } \Gamma \quad (2)$$

where  $K$  is the depth-averaged hydraulic conductivity (assumed isotropic),  $N(\mathbf{x})$  represents natural sources and sinks within the domain,  $f(\mathbf{x})$  represents constant head values imposed on the exterior of the domain,  $\mathbf{x}$  is the spatial coordinates vector,  $\Omega$  represents the problem domain, and  $\Gamma$  represents the domain boundaries. Defining the initial potential function  $\Phi_{\text{init}} = \frac{1}{2}\phi_{\text{init}}^2$  (a common transformation—e.g., Bear [1972], chapter 8), we can recast the steady-state problem in a linear partial differential equation (PDE):

$$N(\mathbf{x}) = \nabla \cdot (K\nabla\Phi_{\text{init}}) \quad \text{on } \Omega \quad (3)$$

with boundary conditions

$$\Phi_{\text{init}} = \frac{1}{2}f(\mathbf{x})^2 \quad \text{on } \Gamma \quad (4)$$

Since  $N(\mathbf{x})$  and  $f(\mathbf{x})$  are both generally poorly characterized due to insufficient measurements of natural sources/sinks and boundary conditions, we seek to eliminate them analytically.

During a pumping test, the modified head field, designated  $\phi_{\text{pump}}$ , satisfies a new equation. Similar to the earlier, we may linearize this new problem defining  $\Phi_{\text{pump}} = \frac{1}{2}\phi_{\text{pump}}^2$ , resulting in:

$$N(\mathbf{x}) + q(\mathbf{x}) = \nabla \cdot (K\nabla\Phi_{\text{pump}}) \quad \text{on } \Omega \quad (5)$$

where  $q(\mathbf{x})$  represents the sources and sinks due to pumping. We then make a key assumption that boundary conditions also do not change during our pumping test:

$$\Phi_{\text{pump}} = \frac{1}{2}f(\mathbf{x})^2 \quad \text{on } \Gamma \quad (6)$$

If a body of water, for example, a river or lake, bounds parts of our domain, then it is generally reasonable to make this assumption. Another reason we may be able to make this assumption is that, if properly designed, a pumping test may have very minor effects on head values at the numerically imposed boundaries.

Finally, we may subtract Equation 3 from Equation 5 and Equation 4 from Equation 6, resulting in:

$$q(\mathbf{x}) = \nabla \cdot (K\nabla\Phi_{\Delta}) \quad \text{on } \Omega \quad (7)$$

subject to:

$$\Phi_{\Delta} = 0 \quad \text{on } \Gamma \quad (8)$$

where  $\Phi_{\Delta} = \Phi_{\text{pump}} - \Phi_{\text{init}}$ . This is now a simple linear PDE (the Poisson equation) subject to homogeneous boundary conditions. The utility of this formulation is that we may now analyze the quantity  $\Phi_{\Delta}$  that is independent of boundary conditions and unknown sinks and sources within the domain. This process is similar to the steady-state drawdown equations used by Li et al. (2008) for an unconfined aquifer, which are also insensitive to boundary conditions and unknown sink/source terms. However, our formulation accounts for the nonlinearity of drawdown with respect to  $K$ , which is expected in unconfined aquifers even under the Dupuit-Forchheimer assumption.

For inverse modeling, it is also important to derive the expected uncertainty in our transformed measurements. We assume that initial water levels are well constrained; thus, our error is due primarily to error in the measurements of head during pumping. Using linear error propagation theory:

$$\mathbf{R}_{\Phi_{\Delta,(i,j)}} \approx \boldsymbol{\varphi}_{\text{pump},(i)} \boldsymbol{\varphi}_{\text{pump},(j)}^T \mathbf{R}_{\phi_{\text{pump},(i,j)}} \quad (9)$$

where  $\mathbf{R}_{\Phi_{\Delta}}$  is the covariance matrix of the transformed measurements,  $\boldsymbol{\varphi}_{\text{pump}}$  is the vector of measured heads during pumping, and  $\mathbf{R}_{\phi_{\text{pump}}}$  is the covariance matrix of head measurements during pumping, and all subscripts in parentheses represent elements of the associated vectors and arrays.

In employing the potential-based analysis method we have suggested, it is important to make sure that any experiments performed and data collected are not adversely affected by our modeling assumptions. For example, measurements of heads at pumping (and injection) wells may be difficult to include since generally significant vertical flow is expected here, thus violating the Dupuit-Forchheimer assumption. Similarly, if tests on an aquifer are expected at steady state to have significant impacts on far-field head values, then assigning boundary conditions becomes problematic.

For our approach, the use of dipole tests or other conservative pumping tests is particularly complementary. It can be shown through analytic modeling (e.g., Strack 1989) that dipole tests at steady state have negligible effects on far-field drawdown. Therefore, even if boundary conditions are not apparent for a particular field problem, they can be imposed at some far-field distance with minimal effect on the near-field solution. Another benefit of this strategy is that more pumping tests are possible. Using simple combinatorics, assuming no measurement at pumping wells, and given  $w$  wells, traditional monopole schemes permit  $w$  pumping tests, each having  $(w - 1)$  measurements. In contrast, dipole tests permit  $\frac{w(w-1)}{2}$  unique pumping tests, each having  $(w - 2)$  measurements. While, in the case of dipole tests, some of these measurements can be seen as collecting “duplicate” information, the addition of extra measurements can be used to cross-validate both the inverted parameter field and the measurement error estimates.

## Inverse Model

During inverse modeling, we solve Equations 7 and 8 numerically for a specific distribution of  $K$  and then compare the modeled values of  $\Phi_{\Delta}$  with the transformed field measurements, which are calculated as  $\Phi_{\Delta}^m = \frac{1}{2}(\phi_{\text{pump}}^m)^2 - \frac{1}{2}(\phi_{\text{init}}^m)^2$ , where the  $m$  superscript denotes measured values of the previously defined quantities. Since our observations are limited in number, and our parameter space is theoretically infinite, the determination of spatially distributed  $K$  is a highly underdetermined problem, and a realistic regularization is necessary.

We use the quasi-linear Bayesian geostatistical inverse method developed by Kitanidis (1995), briefly summarized in this section. Our measurements are assumed to consist of the “true” data plus a multivariate Gaussian error term:

$$\mathbf{y} = \mathbf{h}(\mathbf{s}) + \boldsymbol{\varepsilon} \quad (10)$$

where  $\mathbf{y}$  is an  $n \times 1$  vector of measured data,  $\mathbf{s}$  is an  $m \times 1$  vector of parameter values (in our case, log hydraulic conductivity),  $\boldsymbol{\varepsilon}$  is a zero-mean error term characterized by  $n \times n$  covariance matrix  $\mathbf{R}$ , and  $\mathbf{h}(\cdot)$  is the forward model (mapping from  $\mathbb{R}^m \rightarrow \mathbb{R}^n$  that generates synthetic measurements, given a set of parameters). Our unknown parameter values are assumed to be geostatistically distributed (i.e., spatially correlated) with unknown mean:

$$\mathbf{s} = \mathbf{X}\boldsymbol{\beta} + \boldsymbol{\omega} \quad (11)$$

where  $\mathbf{X}$  is an  $m \times 1$  vector of ones,  $\boldsymbol{\beta}$  is the (unknown) scalar constant mean, and  $\boldsymbol{\omega}$  is a random vector characterized by the  $m \times m$  covariance matrix  $\mathbf{Q}$ , which, in turn, is determined by the spatial arrangement of the unknown parameters and the variogram. The optimum values of the parameters can then be found by optimizing the values of  $\mathbf{s}$  and  $\boldsymbol{\beta}$  using the objective function:

$$\min_{\mathbf{s}, \boldsymbol{\beta}} \frac{1}{2} (\mathbf{y} - \mathbf{h}(\mathbf{s}))^T \mathbf{R}^{-1} (\mathbf{y} - \mathbf{h}(\mathbf{s})) + \frac{1}{2} (\mathbf{s} - \mathbf{X}\boldsymbol{\beta})^T \mathbf{Q}^{-1} (\mathbf{s} - \mathbf{X}\boldsymbol{\beta}) \quad (12)$$

Minimizing this expression is equivalent to maximizing the likelihood of the parameters, given the data under the assumptions of no other informative prior information. For problems where parameters of the measurement error and/or the geostatistics are imperfectly known (as is generally the case), Kitanidis and Vomvoris (1983) give techniques for using empirical Bayesian theory to estimate these “structural” parameters.

For many systems, the above-mentioned inverse problem can be solved through successive linearization by using the following iteration. Starting from the current best estimate of the parameters,  $\tilde{\mathbf{s}}$ , and the linearized forward model (or “sensitivity matrix”),  $\tilde{\mathbf{H}}_{i,j} = \left. \frac{\partial y_i}{\partial s_j} \right|_{\tilde{\mathbf{s}}}$

$$\hat{\mathbf{s}} = \mathbf{X}\boldsymbol{\beta} + \mathbf{Q}\tilde{\mathbf{H}}^T \boldsymbol{\xi} \quad (13)$$

where  $\hat{s}$  is the new best estimate and  $\beta$  and  $\zeta$  are found through solution of the following system:

$$\begin{bmatrix} \tilde{H}Q\tilde{H}^T + R & \tilde{H}X \\ (\tilde{H}X)^T & \mathbf{0} \end{bmatrix} \begin{bmatrix} \xi \\ \beta \end{bmatrix} = \begin{bmatrix} y - h(\hat{s}) + \tilde{H}\hat{s} \\ \mathbf{0} \end{bmatrix} \quad (14)$$

Since our problem is highly underdetermined, we cannot expect that our best estimates of the parameters are perfect. Indeed, many possible parameter fields are consistent with our data, and our best estimate is merely a representation of the features that all “good” parameter fields (as determined by the data) have in common. In order to quantify our uncertainty in the parameter field estimate rigorously, we may examine the posterior covariance of  $s$ , derived as:

$$Q_{ss|y} = Q - \begin{bmatrix} \tilde{H}Q \\ X^T \end{bmatrix}^T \begin{bmatrix} \tilde{H}Q\tilde{H}^T + R & \tilde{H}X \\ (\tilde{H}X)^T & \mathbf{0} \end{bmatrix}^{-1} \begin{bmatrix} \tilde{H}Q \\ X^T \end{bmatrix} \quad (15)$$

The  $m$  diagonal elements of this matrix represent the variances of the individual elements of  $s$  and can be used to visualize our uncertainty in parameter estimates. The posterior covariance estimate above is exact only if the forward model is a linear one—for nonlinear models, the error of parameter values is generally underestimated as the formulation above assumes quasi-linearity in the neighborhood of the optimum  $s$ . The effect of this assumption will be discussed in following sections for specific examples.

## Numerical Example

In order to verify the soundness of our approach, from data transformation to error propagation to numerical modeling, we first tested our routines on a synthetic example problem. The relevant parameters of this synthetic problem are similar to our field experiment (as described in later sections) and can be found in Table 1. The synthetic true parameter field, with regional flow and the location of wells, is shown in Figure 1. Synthetic field data were generated from this model by simulating a series of four dipole (conservative injection/extraction)

Aquifer type	Unconfined
Regional gradient	0.002
Aquifer saturated thickness	16 m
Mean $\log_{10}(K)$	-3.5 (log m/s)
Variogram	$\gamma(h) = .02 \times h$
Number of pumping tests	4
Pumping test type	Dipole at 4 L/s
Number of measurements	28
Parameter discretization	$1 \times 1$ m
Assumed measurement error	2 mm

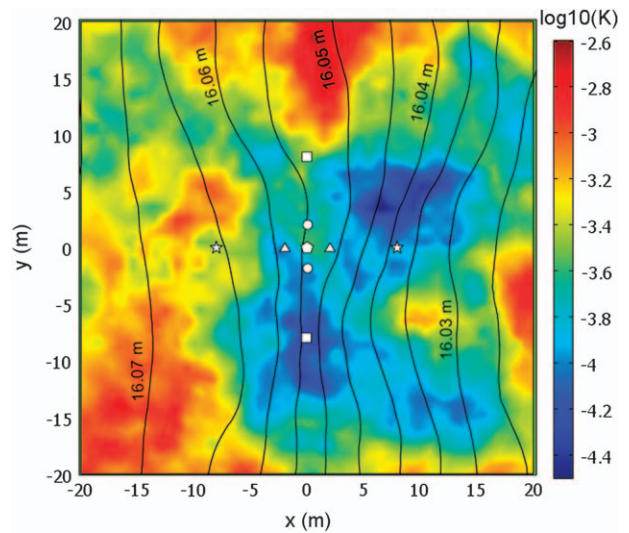


**Figure 1. Synthetic model showing true  $\log_{10}(K)$  field, well locations, and natural preexisting gradient. Contours represent head in m.  $K$  values are in m/s. Well markers show dipoles used in four tests. Test 1 is circles, test 2 is triangles, test 3 is squares, and test 4 is stars. Central well (pentagon) only used for observation during tests and is not pumped.**

pumping tests on this synthetic unconfined aquifer using a depth-integrated Darcy’s law formulation (i.e., 2D subject to the Dupuit assumptions). Observations were generated by evaluating head measurements taken at the nonpumping wells, resulting in seven data points per pumping test. The model used in inversion did not assume knowledge of the true boundary conditions but instead used the Poisson equation for the potential difference with homogeneous boundary conditions—Equations 7 and 8. The inversion consisted of fitting the transformed observations from the synthetic pumping tests— $\Phi'_m$ , as defined earlier—using the Poisson forward model.

For our problem, we implemented our numerical models using COMSOL Multiphysics, a generalized finite-element modeling environment (COMSOL 2005), formerly known as FEMLAB. The inverse problem presented earlier is nonlinear and underdetermined (i.e., fewer observations than unknowns), so we implemented an adjoint state formulation that allows the sensitivity matrix to be calculated in  $O(n)$  time rather than the  $O(m)$  time required by finite difference methods. We used the continuous adjoint state formulation, as described in Sun and Yeh (1990). This technique has been used to study several ill-posed problems—see Yeh and Sun (1990) and Neupauer and Wilson (1999) as examples with lucid descriptions. The details of implementing a continuous adjoint state formulation through COMSOL can be found in Cardiff and Kitanidis (2008).

Results of the inversion, showing the best estimate and posterior uncertainty when using all 28 measurements, are shown in Figure 2. Qualitatively, the true parameter field is reproduced relatively well, especially in the central area bounded by the wells (roughly  $x, y \in [-10, 10]$ ). More quantitatively, we validate these results

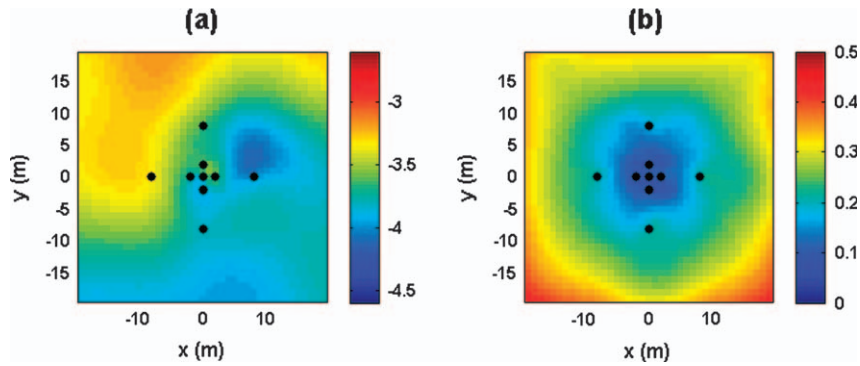


**Figure 2. Results of synthetic inversion using all 28 measurements—(a) best estimate of parameter values and (b) posterior uncertainty estimates.**

in several ways. First, one may examine the normalized errors,  $(\hat{s}_{(i)} - s_{(i)}^{\text{true}})/\sigma_{(i)}$ , as presented in Figure 3, where  $\hat{s}$  is the final best estimate of the parameters,  $s^{\text{true}}$  is the true parameter vector, and  $\sigma_{(i)} = \sqrt{Q_{ss|y(i,i)}}$ . In both the central area, where  $\sigma_{(i)}$  values are relatively smaller (Figure 2b), and the exterior area, where  $\sigma_{(i)}$  values are relatively larger, the normalized residuals appear to be distributed similarly as is expected after normalization. For all four cases, more than 90% of all inverted parameter values fall within 2 standard deviations of the true values and more than 99% fall within 3 standard deviations; this is close to the 95% and 99.7%, respectively, that we would expect if the inversion problem were linear and

shows that uncertainty is not drastically underestimated. While this validation method does not analyze errors in a completely rigorous fashion—for one, it does not consider covariance terms of the errors—it provides a method to visualize errors for multidimensional problems in a way similar to cokriging uncertainty bounds (e.g., Kitanidis 1996; Figure 1). A second way to validate our parameter estimates is to consider our best estimate's ability to reproduce independent (noninverted) test results, as presented in Figure 4. Similarly, we note from this analysis that reproduction of noninverted tests, within computed confidence intervals, appears quite acceptable. Both these analyses indicate that our strategy, including

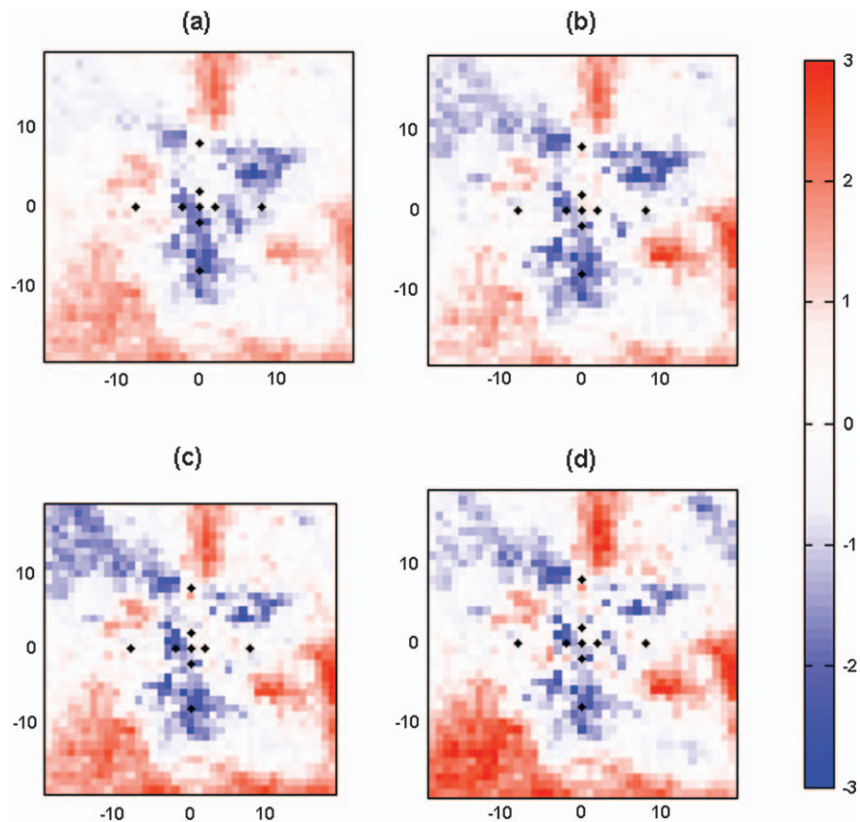


**Figure 3. Normalized parameter estimate errors for the synthetic problem when inverting on (a) 7, (b) 14, (c) 21, and (d) 28 measurements.**

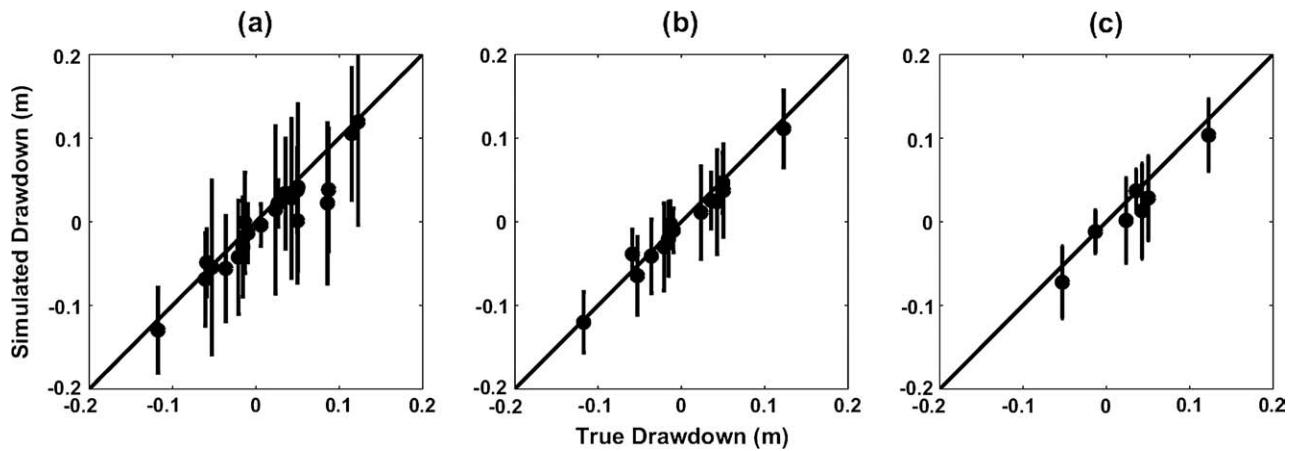


**Figure 4.** Validation of predictive ability of inverted parameter fields. (a) True vs. simulated drawdowns (with 95% confidence intervals) for tests 2, 3, and 4 based on inversion of only test 1 data, and similarly (b) tests 3 and 4 expectations based on inversion of tests 1 and 2 and (c) test 4 expectations based on inversion of tests 1, 2, and 3.

data transformation, linearized error propagation, and quasi-linear uncertainty estimation, gives reasonable best estimates and confidence intervals for our inverted parameter field.

### Application to Field Data

A combined hydrogeophysical study including self-potential, electrical resistivity, and hydrologic (HT) data collection was performed at the BHRS from June 18 to 29, 2007. The primary aquifer stimulation during this study was a series of dipole pumping tests performed using the site's fully penetrating wells. More detailed descriptions of the site, testing design, and field techniques along with raw data and notes from the field experiments can be found in a technical report by Barrash et al. (in preparation) and online at [http://cgiss.boisestate.edu/data\\_downloads/HT\\_data/](http://cgiss.boisestate.edu/data_downloads/HT_data/).

In the following sections, we describe the site setting, data collection, data treatment, and hydraulic tomographic inversion.

### Hydrogeologic Setting and Site Design

The BHRS is a research wellfield in a heterogeneous fluvial aquifer developed by the Center for Geophysical Investigation of the Shallow Subsurface at Boise State University. One purpose of the site was to establish a test bed for the development and testing of minimally invasive geophysical and HT aquifer characterization methods. The BHRS is located at a limited access, uncontaminated natural area adjacent to the Boise River 15 km from downtown Boise, Idaho (Figure 5). The wellfield was designed to permit a wide range of HT and geophysical testing (Barrash et al. 1999; Clement et al. 1999). Eighteen wells were cored through 18 to 21 m of unconsolidated cobble and sand fluvial deposits and completed into the underlying clay. Disturbance of the natural materials near the wells is thought to be minimal based on the drilling and completion methods and subsequent

testing (Morin et al. 1988; Barrash et al. 2006). All wells are 10-cm-inner diameter polyvinyl chloride, are fully screened through the fluvial aquifer, and have blank casing for the uppermost 1.5 m and for well extensions into the underlying clay. Of the 18 wells, 13 wells are concentrated in the 20-m-diameter central area of the BHRS and 5 are "boundary" wells. The 13 wells in the central area are arranged in two concentric rings around a central well, A1 (Figure 5).

Geologically, the BHRS is situated over a sequence of heterogeneous fluvial sediments of the Pleistocene to Holocene, which vary between well-sorted sands of high porosity and more poorly sorted sand and gravel deposits

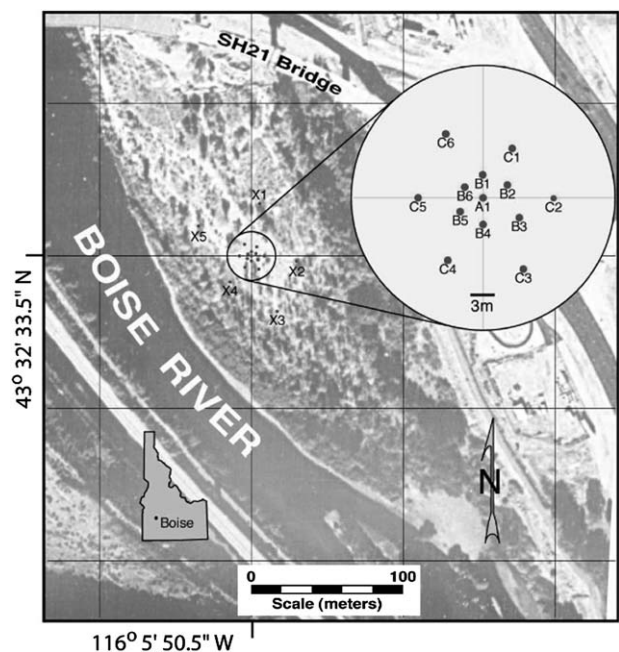


**Figure 5.** Site layout of BHRS showing well arrangement in central area as inset. Diversion Dam is to the southeast on the Boise River.

of lower porosity. Core samples were well recovered from the site ( $\approx 80\%$  recovery from drilling—Reboulet and Barrash [2003]) and suggest at least five distinct units with differing porosity and grain size distributions (Barrash and Clemo 2002; Barrash and Reboulet 2004). Nearby roadcuts and quarry walls suggest complex possibly anastomosing structures, with sand lenses surrounded by massive, poorly sorted gravel-sand mixtures of varying texture.

The site is affected by a number of hydrologic processes. Depth to the water table varies largely with nearby river stage and local topography but is commonly 1 to 2.5 m below land surface. The Boise River stage is very consistent for a given season and is regulated by Diversion Dam and Lucky Peak Dam, which are 0.6 and 4 km upstream of the site, respectively. Site hydrology is affected by evapotranspiration (ET), contributing to a cyclical 1- to 2-cm magnitude daily head variation during the summer months (see figures 38 to 40 in Barrash et al. 2002).

### Test Planning and Operation

A high pumping rate of about 4 L/s was chosen for this highly permeable aquifer ( $K \approx 7.5 \times 10^{-4}$  m/s—estimate from Fox [2006]) in order to produce head changes that were well outside the range of instrument error. Preliminary modeling suggested that a reasonable approximation to steady state would be reached after about 2 to 3 h of pumping, allowing a full set of drawdown and recovery data to be collected once each day.

The number and choice of specific well pairs for the dipole pumping tests were determined using a time constraint of 10 to 12 d and by pretest analytic modeling using an initial homogeneous estimate of  $K \approx 5 \times 10^{-4}$  m/s. By combining analytic solutions for steady-state drawdown in a homogeneous aquifer and the continuous adjoint state formulation, it is possible to analytically derive the sensitivity matrix  $H_{i,j} = \frac{\partial y_i}{\partial s_j}$  for a given set of measurements (see similar analyses for transient

monopole tests in Leven and Dietrich [2006]). Figure 6 shows the results of sensitivity analyses performed with the proposed set of 12 tests. The tests chosen included six cross-site tests (B1-B4, B2-B5, B3-B6, C1-C4, C2-C5, and C3-C6) in addition to six other tests using non-opposite pairs of C wells. Figure 6a is a map of the maximum expected change among all measured values, normalized to a unit log-conductivity change in a unit area of  $1 \text{ m}^2$ —it is computed as the maximum absolute value in each column of the  $H$  matrix. Another perspective on the design's sensitivity is Figure 6b, which is a map of the total expected change in all measurement values, normalized similarly—this is computed as the sum along each column of the absolute value of the  $H$  matrix elements. Overall, our planned tests appeared to “spread” sensitivity adequately throughout the central well area as there are no large regions of low sensitivity within the C well ring.

Hydraulic data were collected throughout pumping and recovery phases using a combination of instruments. Fifteen vented pressure transducers were placed down-well to measure total head change, pseudologarithmically in time, for all wells except X1, X3, and X5 (the wells furthest from the central area). X1 and X5 responses were expected to be relatively slow to develop and thus were measured manually using electric tapes. Well X3 was outfitted with an in-well battery-powered logger for the duration of the experiment to allow continuous collection of both test-related water level changes (on weekdays) in addition to daily ET signals (overnight and during the weekends). Additionally, well A1 was set up with a multilevel packer and port setup (absolute pressure sensor spacing  $\approx 2$  m) in order to collect some depth-dependent pressure change information, also in pseudologarithmically spaced time increments. Boise River stage and river edge positions were measured manually to establish boundary condition control in conjunction with a pressure transducer placed in the river to monitor for possible stage changes during the testing period.

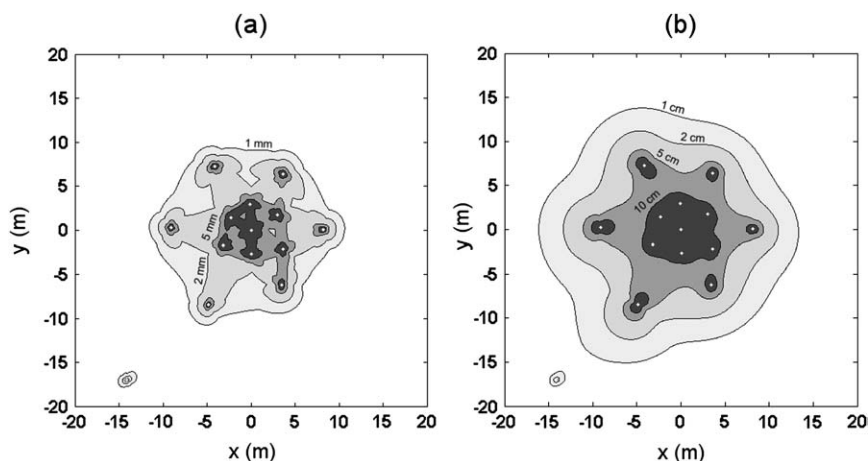


**Figure 6.** Sensitivity map visualization for planned tests using (a) maximum water level change expected due to a unit  $\log_{10}(K)$  change over  $1 \text{ m}^2$  and (b) total water level changes expected due to a unit  $\log_{10}(K)$  change over  $1 \text{ m}^2$  as indicators.

## Field Data

The actual pumping tests performed, which included 9 of the proposed 12 dipole tests and 1 monopole test, are summarized in Table 2. Overall, HT data collected appear reasonable, and the majority of instruments worked as planned. However, due to a failure of the measurement apparatus at X3, long-term observations of ET signals are not available for the time period of our tests. Data from prior years' tests (Figure 7) suggest that ET contributes to a 1- to 2-cm daily head variation. In addition, measurements of water level change at the end of the recovery period—which should have centered around 0 due to the conservative nature of our dipole tests—consistently returned to a negative value indicating overall drawdown at all wells. In order to improve the accuracy of our inversion, which is steady state and thus does not account for ET signals, the effects of this forcing were removed.

Modeling ET as a constant sink term over the problem domain in numerical experiments showed that (for the aquifer saturated thickness, hydraulic conductivity, pumping rates, and ET rates considered) ET can effectively be removed by subtracting a linear trend from all drawdown curves. This is primarily due to the fact that ET-associated changes are very small relative to the saturated thickness. Analysis of ET data from two separate years indicates that ET signals have consistently high (anti-) correlation with temperature data from 2 h prior. Testing during June 2007 generally took place between the hours of 10:00 AM and 4:00 PM. Temperature data during our field experiment were available from the nearby airport, and between the hours of 8:00 AM and 2:00 PM (i.e., 2 h prior to test start and end), the trend in temperature values was consistently linear, also suggesting that subtraction of a linear trend in water level changes from the test data is a good approximation.

Treated, ET-removed versions of the sample test data are found in Figure 8, where a total ET of 1 cm was assumed during the testing period. After trend removal,

the curves appear to closely approximate steady state at the end of the pumping phase (i.e., are very nearly flat). Likewise, the head change at the end of the recovery phase now centers around zero for wells in the target area, as expected from these conservative tests.

## Field Data Analysis and Inversion

For inverse modeling, we developed a numerical model in COMSOL, which assumed a  $60 \times 60$ -m central area of heterogeneity surrounded by a homogeneous field of unknown  $K$ , as shown in Figure 9. Although it is recognized that the area outside of this artificial delineation is actually heterogeneous, the pumping tests performed are only very weakly sensitive to heterogeneities in this outer area. Because our earlier numerical modeling suggested that detection of heterogeneity smaller than about  $1 \text{ m}^2$  (plan view) was infeasible, we discretized our unknown parameter into  $1 \times 1$ -m blocks. The discretization of our forward model (which is finite-element based and independent from the parameter discretization) was set to be very fine near all wells and coarsened toward the far boundaries. This level of mesh refinement and the location of far exterior boundaries were determined by testing simplified COMSOL models against known analytic solutions. For the governing equations of our model, we used the boundary condition- and initial condition-independent Poisson formulation presented earlier and fit the field data using an assumed measurement error of 2 mm. River level data from stage sightings and a pressure transducer indicated that minimal boundary condition changes had occurred during the tests, a requirement for our boundary-independent formulation. Other boundaries necessary for the numerical model were located at least 500 m from the pumping locations, a distance at which dipole tests' effects are negligible. All pumping tests were simulated in the inversion except for test 7, which was a monopole experiment, and test 9, which was a reciprocal pair to test 8 that was not run for as long as other tests

**Table 2**  
**Hydraulic Pump Test Data Available**

Date	Test Number	Extraction Well	Injection Well	Average Flow Rate (L/s)
June 18, 2007	1	B6	B3	3.9
June 19, 2007	2	B1	B4	4.2
June 20, 2007	3	B5	B2	4.1
June 21, 2007	4	C5	C2	4.1
June 22, 2007	5	C6	C3	4.0
June 25, 2007	6	C6	C5	1.7
June 26, 2007	7 <sup>1</sup>	B6	None, monopole	2.3
June 27, 2007	8	C1	C4	4.2
June 27, 2007	9 <sup>1</sup>	C4	C1	4.1
June 28, 2007	10	C4	C3	4.3
June 29, 2007	11 <sup>2</sup>	C5	C1	4.3

<sup>1</sup>Data not used in inversion.  
<sup>2</sup>3D instrumentation removed, and head from transducer in well A1 used.

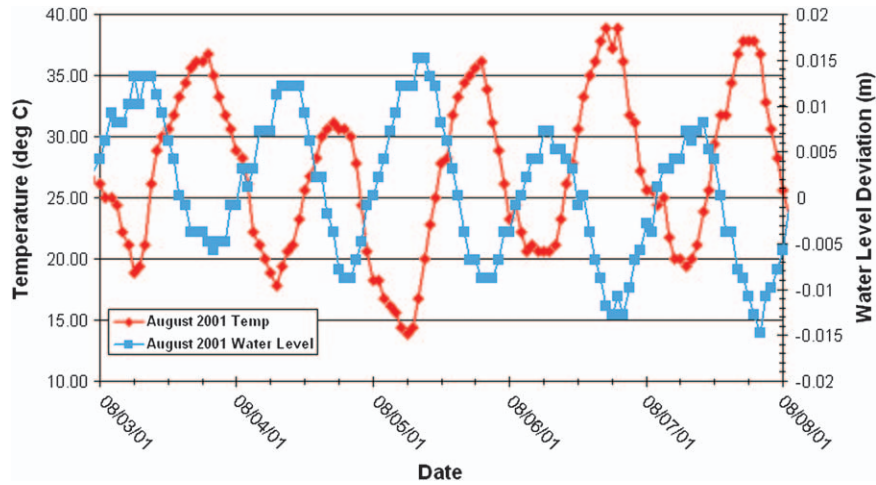


Figure 7. Sample temperature and water level data collected from BHRS in August 2001 (after Barrash et al. [2002]).

and did not approximate steady state. Observations were used from all B wells and C wells, as well as X2 and X4. The responses of well A1 were not included for this 2D model, with the exception of test 11 (which was performed after the packer and port system had been removed from A1). Prior examinations at the site have noted biased parameter estimates when data from the pumping and/or injection wells are used due to skin effects and non-Darcian flow (Barrash et al. 2006; Fox 2006). For this reason, only data from nonpumping wells were inverted.

The final results of our inversion and its posterior error estimates are shown for the BHRS data in Figure 10. These estimates required about 10 h of computing time on a standard desktop PC. During inversion, both the slope and the linear variogram and the degree of epistemic error were optimized using the geostatistical approach of Kitaniadis and Vomvoris (1983). The final epistemic error had a standard deviation of about 4 mm, which is reasonable, given the modeling assumptions invoked and the degree of measurement error of the pressure transducers. The final variogram estimate for  $\log(K)$  determined by the empirical Bayes' theory had a slope of 0.07/m. This

estimate is larger, by more than an order of magnitude, than slopes determined through geostatistical analysis of pseudolocal  $K$  values from analytical modeling by Fox (2006). This is to be expected as it is generally accepted that geostatistics of pseudolocal values of  $K$  from homogeneous analyses drastically underestimate fine-scale variability (Li et al. 2007). Qualitatively, the inverted  $K$  field (Figure 10a) shows largely similar trends to findings from prior published estimates of  $K$  at the BHRS (Fox 2006; Barrash et al. 2006) based on an analytical model that assumes a homogeneous or effective  $K$  value (Moench 1997). In this regard, similarities include (1) relatively greater  $K$  in the southwest and around well C3, which corresponds to the presence of a high- $K$  sand channel in the hydrostratigraphy (e.g., Barrash and Clemo 2002; Barrash and Reboulet 2004; Clement et al. 2006); (2) relatively lower  $K$  in much of the central area (especially around most B wells and C5 and C6), with perhaps an overall NW-SE trend; and (3) a low- $K$  zone localized around well B6 in the central area. The main difference between the modeling presented here and the results from the prior analytical modeling is the relatively higher  $K$  zone along the NE side of the central wellfield (Figure 10a)—which

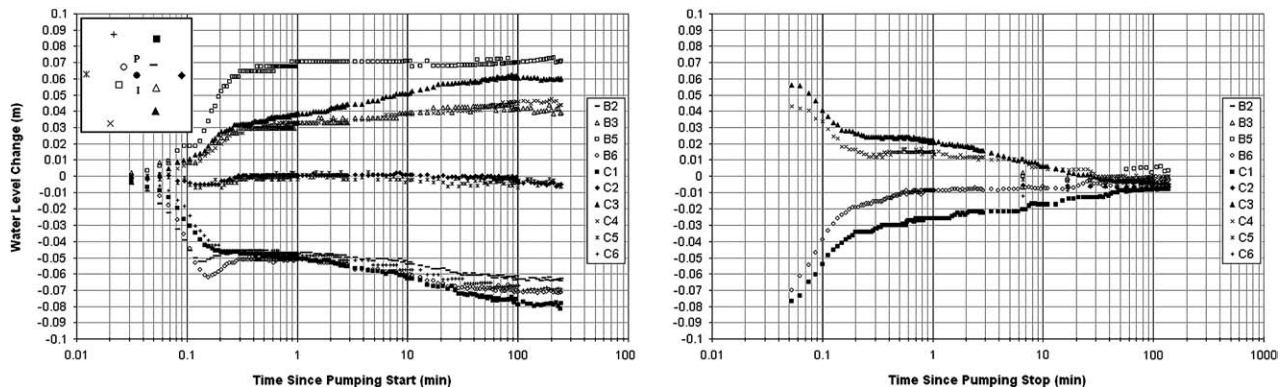
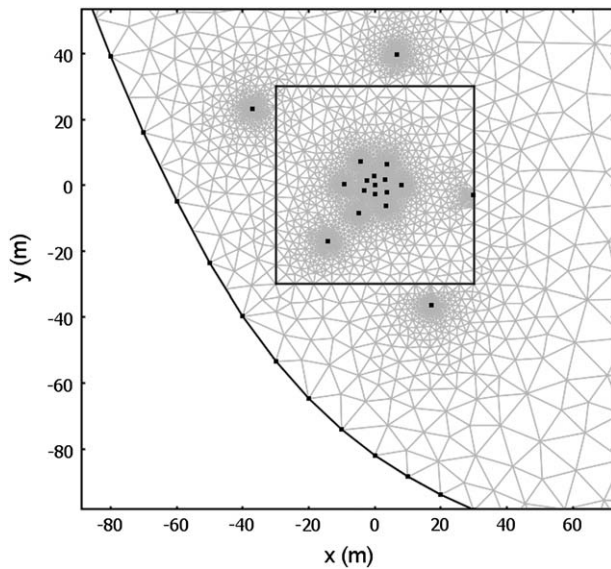
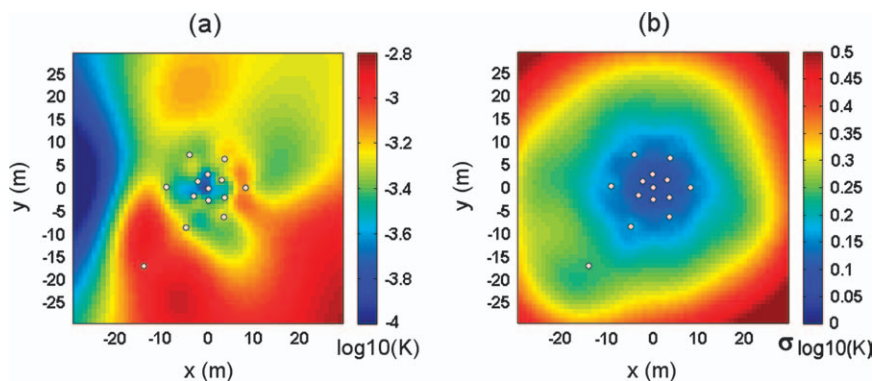


Figure 8. Treated drawdown/buildup data during pump test and recovery phases after removal of ET trend.



**Figure 9.** Close-up of geometry and finite-element mesh for BHRS numerical model (cf. Figure 5). Box shows location of characterized heterogeneous region. Boundary condition to the south and west of A1 (centered at origin) is the Boise River. Other boundary conditions are extended at least 500 m from central area of interest.

also was detected in preliminary (unpublished) modeling of another, less extensive HT dipole data set collected at the BHRS in 2001 but which has relatively lower  $K$  values than the analytical modeling (Fox 2006; Barrash et al. 2006). The error estimates shown in Figure 10b show that, as expected, the use of a homogeneous zone outside of the area  $x, y \in [-30, 30]$  is not particularly detrimental since uncertainty is large as either dimension approaches these outer values. As expected, the sensitivity of the pumping tests is primarily focused near the pumping and observation wells, meaning that while the central area of the site contained by the C well ring is well constrained, it may be necessary to supplement HT data with information from other methods in order to produce reliable maps of heterogeneity outside of this zone.



**Figure 10.** (a) Estimate of  $\log_{10}(K)$  field and (b) estimate of uncertainty in  $\log_{10}(K)$  estimate from inverse modeling of BHRS field HT data. All coordinates are with reference to A1 representing the origin.

## Summary and Conclusions

Modeling of natural systems is inherently a process that may require numerous assumptions while suffering from a sparsity of information. However, by careful design of experiments and analysis of data, we can arrive at results that are not overly affected by our assumptions and that account for the sparsity of information through uncertainty analysis. In this article, we developed a set of equations for modeling unconfined aquifers without perfect knowledge of boundary or initial conditions. Through a combination of this modeling strategy and conservative pumping tests, we believe that steady-state hydraulic tomography can realistically be implemented.

Research on aquifer characterization techniques and methods for inverting HT data has become increasingly exciting and technologically complex in recent years. However, while there is always a need to advance the state of the art (e.g., through 3D HT instrumentation, joint inversion, or parallelized, highly detailed inverse models), we believe there is also a growing need to produce practically useful tools that can reasonably simplify characterization problems and provide realistic results with a relative minimum of computational effort. For many smaller ground water sites, where fully penetrating wells, pumps, pressure transducers, and desktop PCs may represent the sum of available characterization equipment, we believe that simplified techniques such as our potential-based inversion, combined with conservative pumping strategies, may be quite useful.

In the future and as part of continuing characterization efforts, we plan to more fully investigate the utility of our transient field data and the processes that contribute to the temporal drawdown behavior seen. We plan to develop models similar to those presented in this article, which can invert transient data with reduced computational effort. The prevalence of delayed drainage, unsaturated flow, water table dynamics, and the influence of layering and anisotropy will be gauged in order to produce new numerical models that realistically represent the governing physical processes. To help account for these various effects quantitatively, we also hope to

perform future field experiments in which 3D flow can be more reliably imaged through HT (multiple packer and port systems) and geophysical measurements. Last, we plan to integrate the best aspects of HT and geophysical measurements from this field experiment and others using a joint inversion strategy that is appropriate for the unique hydrogeophysical setting of the BHRS.

## Acknowledgments

Mr. Cardiff was funded by the National Science Foundation's (NSF) Graduate Research Fellowship Program throughout the field experiment. Mr. Cardiff's and Dr. Kitanidis' participation in this work was also partially funded by NSF under the grant "Non-equilibrium transport and transport-controlled reactions." The field experiment and participation by Dr. Barrash and Dr. Malama were supported by EPA grants X-96004601-0 and X-96004601-1. Pretest modeling and 2007 HT test design were supported with data provided by, and by discussions with, Dr. Carsten Leven (Helmholtz UFZ, Leipzig, Germany). Significant help during the field experiment was provided by participants in the Boise State/Universita della Calabria (Italy) "Hydrogeophysics Theory, Methods, and Modeling" summer program: Steve Berg, Francesco Chidichimo, Agnes Crespy, Carlyle Miller, Harry Liu, Timothy Johnson, Domenico Sorbo, Leah Steinbronn, and Jianwei Xiang. Finally, the authors would like to thank Olaf Cirpka and Walter Illman, whose comments greatly contributed to the quality of this article.

## References

- Barrash, W., and E.C. Reboulet. 2004. Significance of porosity for stratigraphy and textural composition in subsurface, coarse fluvial deposits: Boise Hydrogeophysical Research Site. *Geological Society of America Bulletin* 116, no. 9: 1059–1073.
- Barrash, W., and T. Clemo. 2002. Hierarchical geostatistics and multifacies systems: Boise Hydrogeophysical Research Site, Boise, Idaho. *Water Resources Research* 38, no. 10: 1196, doi: 10.1029/2002WR001436.
- Barrash, W., T. Clemo, and M.D. Knoll. 1999. Boise Hydrogeophysical Research Site (BHRS): Objectives, design, initial geostatistical results. In *Proceedings of the Symposium on the Application of Geophysics to Engineering and Environmental Problems*, 389–398. Oakland, California: Environmental & Engineering Geophysical Society.
- Barrash, W., T. Clemo, T.C. Johnson, C. Leven, B. Malama, and G. Nelson. 2007. Hydraulic tomography at the Boise Hydrogeophysical Research Site. In *Proceedings of the SIAM Conference on Mathematical and Computational Issues in the Geosciences*. Santa Fe, New Mexico: Society for Industrial and Applied Mathematics.
- Barrash, W., T. Clemo, J.J. Fox, and T.C. Johnson. 2006. Field, laboratory, and modeling investigation of the skin effect at wells with slotted casing, Boise Hydrogeophysical Research Site. *Journal of Hydrology* 326, no. 1–4: 181–198.
- Barrash, W., T. Clemo, D.W. Hyndman, E. Reboulet, and E. Hausrath. 2002. Tracer/time-lapse radar imaging test: Design, operation, and preliminary results. Technical Report BSU CGISS 02–03. Boise, Idaho: Department of Geophysics, Boise State University.
- Bear, J. 1972. *Dynamics of Fluids in Porous Media*. New York: Elsevier Publishing Co.
- Bohling, G.C., J.J. Butler Jr., X. Zhan, and M.D. Knoll. 2007. A field assessment of the value of steady shape hydraulic tomography for characterization of aquifer heterogeneities. *Water Resources Research* 43, no. 5: W05430.
- Bohling, G.C., X. Zhan, J.J. Butler Jr., and L. Zheng. 2002. Steady shape analysis of tomographic pumping tests for characterization of aquifer heterogeneities. *Water Resources Research* 38, no. 12: 1324, doi: 10.1029/2001WR001176.
- Butler, J.J. Jr., C. McElwee, and G. Bohling. 1999. Pumping tests in networks of multilevel sampling wells: Motivation and methodology. *Water Resources Research* 35, no. 11: 3553–3560.
- Cardiff, M.A., and P.K. Kitanidis. 2008. Efficient solution of nonlinear, underdetermined inverse problems with a generalized PDE model. *Computers & Geosciences* 34, 1480–1491.
- Clement, W.P., W. Barrash, and M.D. Knoll. 2006. Reflectivity modeling of ground penetrating radar. *Geophysics* 71, no. 3: K59–K66.
- Clement, W.P., M.D. Knoll, L.M. Liberty, P.R. Donaldson, P. Michaels, W. Barrash, and J.R. Pelton. 1999. Geophysical surveys across the Boise Hydrogeophysical Research Site to determine geophysical parameters of a shallow, alluvial aquifer. In *Proceedings of the Symposium on the Application of Geophysics to Engineering and Environmental Problems*, 399–408. Oakland, California: Environmental & Engineering Geophysical Society.
- COMSOL. 2005. *COMSOL Multiphysics User's Guide*. Version 3.4 ed. Stockholm, Sweden: COMSOL AB.
- Coyt, N., Y. Rubin, and G. Mavko. 1993. Geophysical-hydrological identification of field permeabilities through Bayesian updating. *Water Resources Research* 29, no. 8: 2813–2825.
- Fox, J.J. 2006. Analytical modeling of fully-penetrating pumping tests at the Boise Hydrogeophysical Research Site for aquifer parameters and wellbore skin. M.S. thesis, Department of Geophysics, Boise State University, Boise, Idaho.
- Gottlieb, J., and P. Dietrich. 1995. Identification of the permeability distribution in soil by hydraulic tomography. *Inverse Problems* 11, no. 2: 353–360.
- Hantush, M.S., and C.E. Jacob. 1955. Non-steady radial flow in an infinite leaky aquifer. *Transactions of the American Geophysical Union* 36, no. 1: 95–100.
- Hyndman, D.W., J.M. Harris, and S.M. Gorelick. 1994. Coupled seismic and tracer test inversion for aquifer property characterization. *Water Resources Research* 30, no. 7: 1965–1977.
- Illman, W.A., A.J. Craig, and X. Liu. 2008. Practical issues in imaging hydraulic conductivity through hydraulic tomography. *Ground Water* 46, no. 1: 120–132.
- Illman, W.A., X. Liu, and A.J. Craig. 2007. Steady-state hydraulic tomography in a laboratory aquifer with deterministic heterogeneity: Multi-method and multiscale validation of hydraulic conductivity tomograms. *Journal of Hydrology* 341, no. 3–4: 222–234.
- Kitanidis, P.K. 1996. On the geostatistical approach to the inverse problem. *Advances in Water Resources* 19, no. 6: 333–342.
- Kitanidis, P.K. 1995. Quasi-linear geostatistical theory for inverting. *Water Resources Research* 31, no. 10: 2411–2419.
- Kitanidis, P.K., and E.G. Vomvoris. 1983. A geostatistical approach to the inverse problem in groundwater modeling (steady state) and one-dimensional simulations. *Water Resources Research* 19, no. 3: 677–690.
- Leven, C., and P. Dietrich. 2006. What information can we get from pumping tests? Comparing pumping test configurations using sensitivity coefficients. *Journal of Hydrology* 319, no. 1–4: 199–215.
- Li, W., A. Englert, O.A. Cirpka, and H. Vereecken. 2008. Three-dimensional geostatistical inversion of flowmeter and pumping test data. *Ground Water* 46, no. 2: 193–201.

- Li, W., A. Englert, O.A. Cirpka, J. Vanderborght, and H. Vereecken. 2007. Two-dimensional characterization of hydraulic heterogeneity by multiple pumping tests. *Water Resources Research* 43, no. 4: W04433.
- Liu, S., T.-C.J. Yeh, and R. Gardiner. 2002. Effectiveness of hydraulic tomography: Sandbox experiments. *Water Resources Research* 38, no. 4, doi: 10.1029/2001WR000338.
- Liu, X., W.A. Illman, A.J. Craig, J. Zhu, and T.-C.J. Yeh. 2007. Laboratory sandbox validation of transient hydraulic tomography. *Water Resources Research* 43, no. 5: W05404.
- Luo, J., W. Wu, M.N. Fienen, P. Jardine, T.L. Mehlhorn, D. Watson, O.A. Cirpka, C.S. Criddle, and P.K. Kitanidis. 2006. A nested-cell approach for in situ remediation. *Ground Water* 44, no. 2: 266–274.
- McKenna, S.A., and E.P. Poeter. 1995. Field example of data fusion in site characterization. *Water Resources Research* 31, no. 12: 3229–3240.
- Moench, A.F. 1997. Flow to a well of finite diameter in a homogeneous, anisotropic water table aquifer. *Water Resources Research* 33, no. 6: 1397–1407.
- Morin, R.H., D.R. LeBlanc, and W.E. Teasdale. 1988. A statistical evaluation of formation disturbance produced by well-casing installation methods. *Ground Water* 26, no. 2: 207–217.
- Neupauer, R.M., and J.L. Wilson. 1999. Adjoint method for obtaining backward-in-time location and travel time probabilities of a conservative groundwater contaminant. *Water Resources Research* 35, no. 11: 3389–3398.
- Papadopoulos, I.S. 1965. Nonsteady flow to a well in an infinite anisotropic aquifer. In *Proceedings of Dubrovnik Symposium on the Hydrology of Fractured Rocks*, vol. 73, 21–31. Dubrovnik, Yugoslavia: International Association of Scientific Hydrology Publications.
- Reboulet, E.C., and W. Barrash. 2003. Core, grain-size, and porosity data from the Boise Hydrogeophysical Research Site, Boise, Idaho. Technical Reports 03-02. Boise, Idaho: Boise State University, Department of Geophysics.
- Rubin, Y., G. Mavko, and J.M. Harris. 1992. Mapping permeability in heterogeneous aquifers using hydrologic and seismic data. *Water Resources Research* 28, no. 7: 1809–1816.
- Snodgrass, M.F., and P.K. Kitanidis. 1998. Transmissivity identification through multi-directional aquifer stimulation. *Stochastic Hydrology and Hydraulics* 12, no. 5: 299–316.
- Strack, O.D.L. 1989. *Groundwater Mechanics*. Englewood Cliffs, New Jersey: Prentice-Hall Publishing Co.
- Straface, S., C. Fallico, S. Troisi, E. Rizzo, and A. Revil. 2007. An inverse procedure to estimate transmissivity from heads and SP signals. *Ground Water* 45, no. 4: 420–428.
- Sun, N.-Z., and W. Yeh. 1990. Coupled inverse problems in groundwater modeling. 1: Sensitivity analysis and parameter identification. *Water Resources Research* 26, no. 10: 2507–2525.
- Theis, C.V. 1935. The relation between lowering the piezometric surface and the rate and duration of discharge of a well using ground water storage. *Transactions of the American Geophysical Union* 16, no. 2: 519–524.
- Wu, C.-M., T.-C.J. Yeh, J. Zhu, T.H. Lee, N.-S. Hsu, C.-H. Chen, and A.F. Sancho. 2005. Traditional analysis of aquifer tests: Comparing apples to oranges? *Water Resources Research* 41, no. 9: W09402.
- Yeh, T.-C.J., and S. Liu. 2000. Hydraulic tomography: Development of a new aquifer test method. *Water Resources Research* 36, no. 8: 2095–2105.
- Yeh, W.W.-G., and N.-Z. Sun. 1990. Variational sensitivity analysis, data requirements, and parameter identification in a leaky aquifer system. *Water Resources Research* 26, no. 9: 1927–1938.
- Zhu, J., and T.-C.J. Yeh. 2006. Analysis of hydraulic tomography using temporal moments of drawdown recovery data. *Water Resources Research* 42, W02403.
- Zhu, J., and T.-C.J. Yeh. 2005. Characterization of aquifer heterogeneity using transient hydraulic tomography. *Water Resources Research* 41, no. 7: W07028.